2018-10-30

The minimum inhibitory concentration (MIC) assay with Escherichia coli: an early tier in the environmental hazard assessment of nanomaterials?

Vassallo, J

10.1016/j.ecoenv.2018.06.085
Ecotoxicology and Environmental Safety
Elsevier

The minimum inhibitory concentration (MIC) assay with *Escherichia coli*: An early tier in the environmental hazard assessment of nanomaterials?

J. Vassallo[ab], A. Besinis[acd], R. Boden[ab] and R. D. Handy[ab]

[a]*School of Biological and Marine Sciences, Faculty of Science and Engineering, University of Plymouth, Drake Circus, Plymouth PL4 8AA, UK*

[b]*Sustainable Earth Institute, University of Plymouth, Drake Circus, Plymouth PL4 8AA, UK*

[c]*School of Engineering, Faculty of Science and Engineering, University of Plymouth, Drake Circus, Plymouth PL4 8AA, UK*

[d]*Plymouth University Peninsula Schools of Medicine and Dentistry, University of Plymouth, John Bull Building, Tamar Science Park, Plymouth PL6 8BU, UK*

Correspondence: R.Handy@plymouth.ac.uk

Abstract

There are now over a thousand nano-containing products on the market and the antibacterial properties of some nanomaterials has created interest in their use as cleaning agents, biocides and disinfectants. Engineered nanomaterials (ENMs) are being released into the environment and this raises concerns about their effects on microbes in the receiving ecosystems. This study evaluated the bacterial toxicity of a wide range of nanomaterials with different surface coatings on *Escherichia coli* K-12 MG1655. The minimum inhibitory concentration (MIC) assay, which quantifies the threshold for growth inhibition in suspensions of bacteria, was used to rank the toxicity of silver (Ag), cupric oxide (CuO), cadmium telluride (CdTe) quantum dots, titanium dioxide (TiO_2), nanodiamonds and multi-walled carbon nanotubes (MWCNTs). Bacteria were exposed for 12 h at 37 ^{o}C to a dilution series of the test suspensions in 96-well plates. The precision and accuracy of the method was good with coefficients of variation < 10 %. In terms of the measured MIC values, the toxicity order of the ENMs was as follows: CdTe quantum dots ammonium-coated, 6 mg L^{-1} > Ag nanoparticles, 12 mg L^{-1} > CdTe quantum dots carboxylate-coated, 25 mg L^{-1} > CdTe quantum dots polyethylene glycol-coated, 100 mg L^{-1}. The MIC values were above the highest test concentration used (100 mg L^{-1}) for CuO, TiO_2, nanodiamonds and MWCNTs, indicating low toxicity. The MIC assay can be a useful tool for the initial steps of ENMs hazard assessment.

Keywords: bioassay; ranking test; nanotechnology; tellurium; antimicrobial; metal dissolution

Introduction

Nanotechnology involves the manipulation of materials at the nanoscale in order to infer novel properties (Klaine et al., 2012).While engineered nanomaterials (ENMs) offer many potential benefits to society, there remains a need for safe (Gilbertson et al., 2015) and responsible innovation (Owen et al., 2009). Silver nanoparticles (NPs) are manufactured for their antimicrobial properties and are included in many consumable products (Morones et al., 2005). To date, the predicted environmental concentrations (PECs) of ENMs are low, with values typically in the µg L^{-1} range in natural waters or much less (Lead et al., 2018). In terms of fate and behaviour, particle settling onto soils and sediments is also a concern (Meesters et al., 2016); resulting in the expose of natural microbial biofilms to ENMs.

Microorganisms provide key ecosystem services including aspects of nitrogen and carbon cycles in soils (Coleman et al., 2004). Microbial biofilms also form the base of food webs. Nonetheless, most of the available studies on the antibacterial effect of ENMs have used clinical isolates, including clinical strains of *Escherichia coli* and *Bacillus subtilis* (Yoon et al., 2007), as well as *Streptococcus aureus* (e.g., Xiu et al., 2014). For example, median minimum inhibitory concentrations (MICs) values of 7.1 mg L^{-1} and 200 mg L^{-1} have been reported for *E. coli* exposed to silver and cupric oxide NPs respectively (Bondarenko et al., 2013). Such laboratory studies show different degrees of bacterial sensitivity depending on the organisms and the type of ENM, but the mechanisms that cause it are not yet clear; although both contact toxicity and free ion toxicity have been suggested for Ag NPs (review by Reidy et al., 2013).

It was originally thought that the primary habitat of *E. coli* was the gut of host animals and humans; with faecal releases being an incidental route for the microbe to enter the environment. In fact, 'naturalised' strains of *E. coli* occur widely in soil and water (Winfield and Groisman, 2003). In the environment, *E. coli* retains its facultative adaptability and can process a range of soil nutrients including carbon, nitrogen, phosphorus and sulfur (Brennan et al., 2013). It is therefore an integral part of the natural microbiome. However, the effects of ENMs on microbial biodiversity in real ecosystems, or in complex biofilms, remains unclear. Additions of 1 mg L^{-1} of silver NPs to the overlying water showed no effects on microbial biodiversity of estuarine sediment (Bradford et al., 2009). In an investigation of silver and aluminium oxide NPs effects on soil microbes, a shift in soil microbial biodiversity was not observed, but changes to the microbial gene expression profile were detected (Fajardo et al., 2014).

While there remains some uncertainty around the environmental consequences of ENMs on microbial ecosystem services, these organisms are nonetheless widely used in regulatory testing for environmental hazard assessment (review by Crane et al., 2008). These include the Organisation for Economic Co-operation and Development (OECD) 301, OECD 302A, 302B, 302C and OECD 308 biodegradation-related tests, as well as assays to measure microbial carbon and nitrogen transformation in soils (OECD 216 and 217 respectively, see Crane et al., 2008). Bacteria are also used incidentally for genotoxicity assessment due to their rapid cell division (e.g., in the Ames test), but there is no acute ecotoxicity test for bacteria exposed to chemicals, or ENMs *per se* in the OECD testing strategy for the environment. A rapid tool would be especially useful to provide an early demonstration of microbial ecotoxicity of ENMs and to rank ENMs of concern.

At present, regulatory ecotoxicity testing requires each new chemical substance to be tested individually for hazard, including ENMs. There are some suggestions to rationalise testing, including comparing ENMs with their nearest existing approved chemical substances (Crane et al., 2008), and read-across approaches to deal with ENMs with surface coatings (Oomen et al., 2014). Nonetheless, despite suggestions for amending the environmental testing strategy for ENMs (Handy et al., 2012), the strategy remains expensive and laborious; but critically also without a ranking tool that can be used to reduce the burden of regulatory work in an ecological context. In addition, difficulties arise when one attempts to compare the results of toxicity tests conducted on bacteria with ENMs, as no common testing protocols are being used in microbial ecotoxicology research (different types of growth media, test suspension preparation methods, test vessels, test duration and dosing, etc.,). For product screening and regulatory ecotoxicology, a standardised protocol that is robust and reproducible is therefore desirable.

There is a microbial toxicity test that has been standardised for the pharmaceutical industry. The minimum inhibitory concentration (MIC) assay is the most commonly used technique in the pharmaceutical testing of bactericidal activity (Wiegand et al., 2008). Specifically, the broth dilution method consists of a bacterial inoculation in a liquid growth medium, in the presence of different concentrations of the drug or antibiotic under test. This test has been recently adapted for clinical samples of the oral pathogenic species *Streptococcus mutans* in the presence of silver, silica and titanium dioxide ENMs (Besinis et al., 2014), but its utility as a simple routine environmental test with *E. coli* and with a range of ENM chemistries has not yet been explored.

The primary aim of this study was to demonstrate the usefulness, from a nano-ecotoxicological perspective, of adopting the MIC assay for testing a range of ENMs with different chemistries under standardised exposure conditions to facilitate regulatory use. *Escherichia coli* K-12 MG1655 was chosen for the environmental reasons outlined above, but also because this strain is a model (Reinsch et al., 2012) for measurements of bacterial biomass and growth yields. A secondary aim was to evaluate any differences in the bacterial response to the presence of uncoated or coated (functionalised) ENM variants: carboxylate (-COOH), amine ($-NH_2$), ammonium ($-NH_4^+$) and polyethylene glycol-coated types. Microscale (bulk) material counterparts or metal salts, as appropriate, were also tested.

Methods

Culture of microorganisms

The bacterial strain *Escherichia coli* K-12 MG1655 (DSM 18039) (Migula 1895) Castellani and Chalmers 1919 was purchased from the Leibniz Institute - Deutsche Sammlung von Mikroorganismen und Zellkulturen GmbH. This derivative of the K-12 strain has been cured of plasmids, virulence factors and phages (Guyer et al., 1981) and thus gives more consistent behaviour *in vitro*. It also has a high specific growth rate, μ (Hayashi et al., 2006).

In order to obtain reproducible inocula (Pirt, 1967), 10 mL nutrient broth was inoculated with a colony from a 24 h old nutrient agar slant. Subsequently, a 500 mL batch culture of *E. coli* K-12 MG1655 was grown for 12 h, then harvested by centrifugation at 4 ^{o}C, 10,000 x *g* for 30 min, washed and suspended in sterile saline (0.90 % (*w/v*) NaCl). This culture was diluted to a final optical density (*OD*) at 440 nm *c.* 0.90 (Jenway 7315 UV/Visible Spectrophotometer) and stored at - 80 ^{o}C until required for the experiments. The wavelength selected for *OD* calibration has a linear response of high sensitivity for short rods without any interference from the Soret peak of cytochrome *c* (Boden et al., 2010).

Experimental approach and the MIC assay

The current study investigated the toxicity of the following ENMs: silver metal (Ag); cupric oxide (CuO); cadmium telluride quantum dots (CdTe QDs); spherical and tubular forms of titanium

dioxide (TiO_2); nanodiamonds and multi-walled carbon nanotubes (MWCNTs), as compared to the equivalent metal salts or bulk controls. Mercuric chloride was used as the positive control for toxicity. The materials were uncoated and coated (functionalised) ENM variants as follow: carboxylate (COOH), amine (NH_2) / ammonium (NH_4^+), or polyethylene glycol (PEG) functionalised ENMs for negative, positive and neutral surface functionalisation respectively. The precise details of how the coatings were synthesised and attached to the ENM core is commercially sensitive information of the suppliers, but for clarity we use the term '$–NH_4^+$' to mean an $–NH_3$ terminal ligand that has been ionised with H^+ ions to achieve positive charge. The hypothesis was that uncoated ENMs may lead to observable toxicological effects, and that the surface-coatings of the ENMs may also influence the resulting toxicity. Ultrasound (sonication) was not used while preparing the test suspensions in order to prevent the detachment of the ENMs surface coatings from the uncoated materials and to avoid any possible ultrasonic-induced chemical changes to the test materials (Taurozzi et al., 2010). Critically, this approach also simplified the method for use as a standard regulatory test.

The minimum inhibitory concentration (MIC) assay allows the determination of the minimum dilution of a test suspension that gives complete inhibition of bacterial growth. The MIC assay experimental design is depicted in Supplemental Figure S1 with $n = 6$ replicate test plates. Initial experiments were also carried out in Erlenmeyer flasks to compare growth to that in 96-well plates. Growth was confirmed to be satisfactory in both test-vessels, although less absolute growth measured in 96-well plates (data not shown). Nonetheless, in the final protocol reported here, 96-well plates were chosen for their convenience over flasks.

In this work, analytical grade reagents or better were used. The E-basal salts (EBS) (Kelly and Syrett, 1964; Tuovinen and Kelly, 1973) as modified by Boden et al. (2008) was used as a minimal defined medium. This medium was also chosen as the least likely recipe to cause aggregation of ENMs in suspension. It was supplemented with 10 mM D-(+)-glucose (Sigma, ≥ 99.5 % purity) as the sole carbon and energy source. During the actual exposures in 96-well plates, test suspensions/solutions were diluted with the growth medium and the inoculum; with the resultant exposure medium referred to hereafter as 'NaCl-EBS medium'. In this study, the term 'test suspension' or 'stock suspension' refers to the dispersion of ENMs or micron scale particles in a liquid, whereas the phrase 'test solution' refers to metal salts or other soluble substance in solution.

The final optimised MIC protocol for the experiments involved pipetting 200 µL of each test suspension/solution, at nominal concentrations ranging from 1.5 to 100 mg L^{-1} (prepared by serial dilution, see below), into 96-well microplates (flat-bottom sterile polystyrene, 0.415 mL capacity, Fisher brand) containing 20 µL of 10x strength EBS (sterilised just before plating, 0.2 µm Minisart Plus filter) and 22 µL of the inoculum above. Abiotic controls were run in parallel on each plate to account for the turbidity effect of the saline solution and for the turbidity caused by the test suspension or solution. A set of normal growth controls for growth in the absence of any test suspensions and positive controls (mercuric chloride, Sigma, 99 % purity) for complete growth inhibition (Boden and Murrell, 2011) were included. The 96-well plates were incubated (New Brunswick Scientific Model G25, Edison, USA) for 12 h at 37 °C. The plates were allowed to shake at 130 rpm during the exposure period to ensure aerobic conditions in the medium. After the exposure period, the contents of the plates were pipette-mixed to re-suspend any material which may have deposited to the bottom of the wells. Immediately afterwards, OD_{440} was measured to determine growth using VersaMax microplate reader with SoftMax Pro 4.0 software (Molecular Devices, Sunnyvale, CA, USA), and appropriate correction for the turbidity controls. Glucose and carbon consumption were also determined (see below).

Test suspension preparation and characterisation

In order to clean and deionise glassware, all media bottles and glass stirring rods were washed overnight with 5 % (*v/v*) nitric acid (Fisher, Primer Plus Trace Metals Grade) trace analysis grade and rinsed three times with glass distilled water (distilled from ion-free ultrapure water, 18 MΩ resistance), then autoclaved for a 15 minute cycle at 121 °C and 15 psi. A sterile 1 g L^{-1} test suspension or solution, as appropriate of each material, was prepared by weighing 0.05 g (Sartorius BP 210) of powder and added to 50 mL of sterile glass distilled water. For metal salts, the amount of powder weighed was adjusted to account for the relative mass contribution of the metal species in the uncoated ENMs and bulk controls. All stock suspensions or solutions were stirred for 3 h (IKA-WERKE R015), set at speed 3. Then, a 1:10 dilution of the stock in sterile physiological saline (0.90 % NaCl) was prepared to achieve a working nominal concentration of 100 mg L^{-1}. The use of the saline prevented osmotic stress to the test organism during the exposures, while enabling a suitable dilution for the experiments. Subsequently, by a 50 % serial dilution in 0.90 % NaCl to the following nominal concentrations were made: 50, 25, 12, 6, 3, and 1.5 mg L^{-1}. Each

196 test suspension or solution was vortexed (Minishaker MS2 IKA) in between dilution steps to
197 ensure homogeneity of the liquid for pipetting.
198 Details of the purity, primary particle size and surface area of the materials investigated are
199 found in Table 1; together with the measured mean aggregate size and mean particle concentration
200 in 0.90 % NaCl. Particle number concentration and particle size distribution in the 100 mg L^{-1}
201 nominal test suspensions were measured by nanoparticle tracking analysis (NTA) using a
202 Nanosight LM 10 (Malvern Instruments, UK). Three sub-samples from each of the fresh stock
203 suspensions (10 mL each) were vortexed for 10 s immediately before analysis. A capture
204 timeframe of 10 s was used, with shutter and gain settings of 1390 and 200 respectively. Particle
205 size distributions are reported as the particle number concentration, along with the hydrodynamic
206 diameter in Table 1.
207
208 ***Dissolution of ENMs in the exposure media***
209 The degree of metal ion dissolution in the NaCl-EBS medium was determined for silver, copper,
210 cadmium, tellurium, and titanium containing materials by dialysis following the method of Besinis
211 et al. (2014). These experiments were conducted at room temperature, pH 6.5, and with dialysis
212 tubing with a molecular weight cut off 12 kDa (Sigma). The latter with a measured pore size by
213 electron microscopy in our laboratory of < 2 nm. Dialysis bags were filled with 8 mL of the
214 appropriate 100 mg L^{-1} nominal test suspension or solution, and suspended in a 600 mL beaker
215 containing 492 mL of the medium (in triplicate beakers). The experiments were consistently
216 carried out under slow agitation, using a magnetic plate stirrer. Blanks with no test suspensions
217 added to the dialysis bags were also included in each experiment. Samples of media (1 mL) were
218 taken from the external compartment of the beaker at time zero, 30 min, 1, 2, 3, 4, 6, 12 and after
219 24 h. Samples were acidified by addition of 4 mL of 5 % (*v/v*) nitric acid. Samples of 0.5 mL media
220 were also taken at each time point for pH measurements (Thermo Scientific Orion 2-Star Plus
221 meter fitted with a Russell combination electrode). The contents of the dialysis bags were sampled
222 both at the start (i.e., the stock used to fill it) and end of the experiment. The total metal
223 concentrations of all the samples were analysed by inductively coupled plasma optical emission
224 spectrophotometry (ICP-OES) or by inductively coupled plasma optical mass spectrophotometry
225 (ICP-MS) using the Thermoscientific, X Series 2 (see below).
226

227 ***Total metal analysis***

228 Total metal concentrations of silver, copper, cadmium, tellurium, titanium and mercury (Table 1)
229 were measured in the NaCl-EBS medium using ICP-OES (Thermo Scientific, iCAP 7000 series).
230 Prior to analysis, all samples were diluted 1:5 with 5 % (*v/v*) nitric acid. For titanium concentrations
231 a 2:1 mixture of concentrated sulfuric acid to nitric acid (analytical grade reagents) was used
232 (Mudunkotuwa et al., 2016). Acidified, matrix-matched ICP-OES standard metal solutions were
233 used for calibrations and with sample blanks included every 10 samples in each run of the
234 instrument. Internal standards of yttrium or indium were also included to correct for instrument
235 drift during the analyses (Shaw et al., 2013).

236

237 ***Glucose determination***

238 The concentration of unconsumed glucose in the plates was measured (GO-20 assay kit, Sigma)
239 at the end of each experiment to ensure that growth had not been limited by the absence of glucose
240 and/or loss of bioavailable glucose in the suspensions. The kit was used according to the
241 manufacturer's instructions. The assay employs glucose oxidase to oxidise the glucose to gluconic
242 acid and hydrogen peroxide. The latter reacts with a colour reagent to from a stable pink colour
243 which is proportional to the original glucose concentration. Briefly, 140 µL of the remaining
244 volume from each experimental well, both test and control wells, were transferred to V-bottom
245 microplates (V-bottom sterile polystyrene, 0.415 mL capacity, Fisher brand) which were
246 centrifuged (2000 rpm for 10 min with a 2040 Rotors microplate centrifuge, Centurion Scientific
247 Ltd, Ford, UK) to pellet the particles and the bacteria. Then, 4 µL of the supernatant from each of
248 the wells were removed to new flat bottom 96-well plates, and diluted with 36 µL of water.

249

250 ***Biomass and growth yield determination***

251 The correlation between *OD* at 440 nm and amount of biomass produced was determined from
252 calibration curves prepared from suspensions of *E. coli* K-12 MG1655, diluted to various optical
253 densities with spent culture and dried to constant weight at 85 ^{o}C. An OD_{440} of 0.1 was
254 experimentally found to correspond to 14 mg dry biomass L^{-1} (data not shown). The growth yield
255 (Y_C) as grams dry biomass per mole of carbon consumed was determined from the biomass
256 produced and glucose consumed:

$$Y_C = \frac{\Delta\, biomass}{\Delta\, glucose}$$

Statistical analyses

Statistical analyses were carried out using IBM SPSS Statistics version 21. Following descriptive statistics, the Kolmogorov test was used to check for normality. Independent student *t*-tests and one-way analysis of variance (ANOVA, Tukey *post hoc* test) were used to check for significant differences amongst responses from within each test material and treatments (e.g., comparing absolute growth to each dilution effect) and then amongst treatments for the same material chemistry type (e.g., comparing percentage relative growth for carboxylate, ammonium, polyethylene glycol-coated nanodiamonds). All statistical analyses used a 95 % confidence limit, so that p values ≥ 0.05 were not considered statistically significant. The data are shown as mean ± standard error of the mean (S.E.M). The coefficient of variation expressed as a percentage was sometimes used to show the variability amongst plates for each test concentration and treatment. Dissolution curves were fitted using SigmaPlot version 12.5 by applying the hyperbola, single rectangular, 2 parameter equation on the raw data points.

Results

Behaviour of the nanomaterials in the test media

Incidental visual observations during the preparation of the stock dispersions identified that some materials tended to aggregate in the high ionic strength of the 0.90 % NaCl. There were some size effects with the Ag and CuO NPs appearing dispersed, whereas their micron scale counterparts (colloid silver, bulk CuO) tended to settle onto the bottom of the plates. There were also some apparent differences in the behaviour of the ENMs, depending on the coating. For example, the uncoated CuO and CuO-NH_4^+ ENMs appeared well dispersed, whereas the CuO-COOH and CuO-PEG formed observable black aggregates in 0.90 % NaCl. In contrast, the coating effect was not the same for the CdTe QDs materials, with the CdTe-NH_4^+ form changing to a greyish colour and sinking as visible aggregates. Visually, the nanodiamonds appeared as a good dispersion in 0.90 % NaCl, regardless of surface coating. Of the MWCNTs, the uncoated form proved to be more difficult to disperse in 0.90 % NaCl forming observable large aggregates.

The level of dispersion of the materials in 0.90 % NaCl was confirmed by NTA measurements of the hydrodynamic diameters and particle number concentrations (Table 1). In 0.90 % NaCl much larger hydrodynamic diameters than those reported in the manufacturers' information for the primary particle size were determined. For example, dry powders of the CdTe QDs had diameters in the 3 – 5 nm range, in contrast to much larger sizes (> 50 nm) as measured by NTA in 0.90 % NaCl (Figure 1a-c). The particle number concentrations in the dispersions of ENMs also generally decreased with the hydrodynamic diameters, consistent with some particle aggregation and settling in 0.90 % NaCl.

In terms of comparing ENMs with their micron scale counterparts, the larger hydrodynamic diameters were, as expected, mainly observed for the microscale materials (Table 1). For example, for Ag NPs the mean hydrodynamic diameter was less than 100 nm, but almost 200 nm in the micron scale colloidal silver equivalent (*t*-test, $p > 0.05$). However, the effect of ENM coatings on the mean hydrodynamic diameter was material-specific (Table 1). For example, the uncoated CuO ENMs (182 nm) showed no statistical significant difference in size relative to the coated forms of CuO NPs (ranges 120 – 140 nm for the coated CuO ENMs, ANOVA, $p > 0.05$). Particle size order as hydrodynamic diameters of CdTe coated QDs were also measured by NTA. Particle size by QD coating type increased in the following order: $-NH_4^+$, -COOH and -PEG, with the ammonium and carboxylate forms (< 100 nm) statistically significantly smaller (ANOVA, $p < 0.05$) than the PEG form (> 150 nm); and bulk CdTe (> 100 nm) not different overall in particle size to that of the QDs (ANOVA, $p > 0.05$).

Confirming exposure in the NaCl-EBS medium

In addition to checking the state of dispersion and metal concentrations in the initial 0.90 % NaCl stock dispersions and solutions. Attempts were also made to measure the total metal concentrations in the NaCl-EBS medium at the start of the experiment compared to the expected nominal concentrations where relevant (Table 1). For the metal salts, the measured values were within 80 % of the nominal concentrations. For example, the measured concentrations as a percentage of the calculated total metal concentrations were: 88 % copper in $CuSO_4$, 79 % cadmium in $CdCl_2$, 98% tellurium in K_2TeO_3 and 91 % Hg in $HgCl_2$. The only exception to this was $AgNO_3$, which is known to form insoluble silver chloride particles in saline media, and thus the apparent dissolved silver was around 10 % of the expected nominal value. For all ENMs where measurement was

possible, the presence of total metal was confirmed. However, the measured metal concentrations in the NaCl-EBS media was less than the calculated total metal concentrations for the ENMs, with (% of nominal value): 5 % for Ag NPs; > 85 % for CuO NPs, 50 – 70 % for cadmium and tellurium in QDs; and 30 – 60 % for TiO_2-based ENMs. Similarly, for the bulk powders, the measured metal concentration were less than nominal, but still a readily detectable concentration that confirmed exposure had occurred (Table 1).

Dialysis experiments and release of total dissolved metals into NaCl-EBS medium

The total dissolved metal concentrations in the NaCl-EBS medium were measured over 24 hours during dialysis of the materials where it was technically possible. The maximum apparent dissolution rates were also calculated from the steepest initial phase of each dialysis curve (Table 1). Example dialysis curves are shown in Figure 2. The dialysis bags were filled with a total of 800 µg of each material, and yet the maximum dissolution rates were either at or below detection limits, or around 1-3 µg min^{-1} for most substances (Table 1). Maximally, this equates to round 0.1 - 0.4 % of the metal in the material min^{-1}.

Silver regardless of form, showed the least release of total dissolved metal into the external compartment of the beakers compared to all the other metals tested, and with the lowest apparent initial dissolution rates (Table 1). After 12 h, both the bulk and the nano forms of silver showed some detectable metal concentrations in the external medium, but this remained low with no statistically significant differences between these materials (ANOVA, $p > 0.05$, Figure 2a). Of the substances made of silver, only the $AgNO_3$ showed a clear time-dependent appearance of total silver in the external media of the beaker (Figure 2a), being statistically higher than with the Ag ENMs or Ag bulk material by 12 hours (ANOVA, $p < 0.05$, Figure 2a).

Contrasting with the silver, the Cd and the Te metal salt controls as expected showed some solubility in the media, with the highest initial slopes on the dialysis curves of around 6 µg min^{-1} (Table 1, equating to ~0.8 % min^{-1}). There were some material-type effects in relation to Cd and Te. The CdTe-QDs, regardless of coating, released less dissolved metal than the equivalent metal salts (Table 1, Figure 2b, c). There were also some small, but statistically significant coating effects, within the CdTe-QDs for the final total dissolved Cd concentrations in the beakers; with less Cd released from the CdTe-PEG material (ANOVA, $p < 0.05$, Figure 2b). Notably, this pattern in the coating effect for CdTe-QDs was not the same for the Te metal concentrations in the beakers,

with the Te concentrations being in the order: COOH > PEG > NH_4^+ (Figure 2c); with the measured Te concentration being lower (ANOVA, $p < 0.05$, Figure 2c) in the beakers for the NH_4^+ compared to the other coatings. The CdTe bulk material was even less soluble than the ENMs with no detectable increases of either Cd or Te metal concentrations in the beakers (Figures 2b and 2c).

Copper sulfate, like the Cd salt, caused some appearance of total dissolved metal in the external media of the beakers, although the rate of appearance of Cu was around 3 µg min^{-1}, approximately half that of $CdCl_2$ (Table 1). Similar to the findings with the CdTe materials, the CuO ENMs also showed some dissolution, but much less than the equivalent metal salt, and with the bulk CuO material showing the lowest Cu concentrations in the external media of the beaker (Table 1, Figure 2d). In terms of a coating-effect within the CuO ENMs (Figure 2e), there were some initial differences with faster appearance of Cu in the beakers from the CuO-COOH material, but this effect was lost within 6 hours, and thereafter no coating effect was observed for total Cu from the CuO ENMs (Figure 2e). Regardless of coating or not, the $CuSO_4$ gave the highest Cu concentrations in the beakers at the end of the experiment (ANOVA, $p > 0.05$, Figure 2d).

Minimum inhibitory concentration assay

Escherichia coli K-12 MG1655 in the absence of test materials showed normal growth, with a growth density of about 40 mg dry weight biomass per litre; whereas the positive control for toxicity (mercuric chloride), as expected, prevented growth at all the tested dilutions. Figure 3 shows the effect of the different test suspensions on bacterial growth using the MIC assay. The coefficient of variation (CV) indicated generally good reproducibility of this assay. The normal growth controls had a grand CV (average ± S.E.M, $n = 336$) of 6.1 % ± 1.0. The CV for the different materials were generally 10 % or much less, and summarised as follows by chemical substances: silver < 4 %; copper < 10 %; CdTe < 6 %; TiO_2 < 9 % and nanodiamonds < 5 %. The most variability was seen for the MWCNTs (24.9 % ± 2.7), especially at the highest test concentration.

The MIC values obtained from the growth curves are shown in Table 2. For several ENMs, even with a nominal exposure of 100 mg L^{-1} no effects on growth were observed; or were modest at one or two of the higher exposure concentrations such that an MIC value could not be determined. This was the case for ENMs of cupric oxide, titanium dioxide, nanodiamonds and MWCNTs (MIC values above the maximum concentration used in the test, Table 2). However,

379 some of the CdTe and silver ENMs showed toxicity with a ranking as follows for the MIC when
380 toxicity was observed in the experimental conditions used here: CdTe QD-NH_4^+ > Ag NPs > CdTe
381 QD-COOH > CdTe QD-PEG. Of the metal salts, $AgNO_3$ was consistently as inhibitory to *E. coli*
382 K-12 MG1655 as mercuric chloride at all the concentrations tested (Figure 3a) and achieved the
383 same MIC value as mercury (Table 2). Both $CuSO_4$ and $CdCl_2$ showed limited toxicity with MIC
384 values greater than 100 mg L^{-1}. The K_2TeO_3 salt was slightly more toxic with an MIC value of
385 around 50 mg L^{-1} (Table 2).
386 In terms of material-type effects on bacterial growth, the Ag NPs were not as effective as
387 $AgNO_3$, but nonetheless a nominal concentration of 12 mg L^{-1} of Ag NPs or higher completely
388 inhibited growth (Figure 3a). The micron scale Ag powder (colloidal silver) had limited biocidal
389 properties and less than the nano form, with complete growth inhibition seen from 50 mg L^{-1} or
390 higher for colloidal silver. No particle coating experiments were performed with silver because
391 coated versions of the Ag NPs were not available. For copper (Figure 3b), there was no growth
392 difference for *E. coli* K-12 MG1655 between the bulk CuO and the uncoated CuO ENM from 1.5
393 to 50 mg L^{-1} nominal concentrations. However, at the highest test concentration (100 mg L^{-1}) a
394 material-type effect emerged with the bulk CuO stimulating bacterial growth, whereas the
395 uncoated CuO ENM reduced the bacterial viability by approximately 20 % compared to the normal
396 growth control (ANOVA, $p < 0.05$). For $CuSO_4$ exposure, statistically significant reductions in
397 growth relative to the unexposed controls (ANOVA, $p < 0.05$) were only observed at nominal
398 concentrations of 50 and 100 mg L^{-1}, with reductions of 20 and 50 % respectively (Figure 3b). The
399 $CuSO_4$ was more toxic than the bulk CuO and of similar toxicity to the uncoated CuO ENM at the
400 highest test concentration. However, there was no observable coating effect within the ENMs as
401 none of the coatings showed growth inhibition.
402 The cadmium salt and the bulk CdTe equivalent to the quantum dots were not toxic to *E.*
403 *coli* K-12 MG1655 (Figure 3c). For reasons related to the synthesis of the QDs there is no uncoated
404 material. All the coated CdTe QDs studied were found to reduce bacterial viability, with growth
405 inhibition being most severe in the presence of the ammonium coated QDs, followed by the
406 carboxylate and PEG-coated forms. The tellurium metal salt displayed a linear concentration-
407 related growth inhibition effect ($r^2 = 0.96$) up to the 25 mg L^{-1} nominal concentration; and complete
408 growth inhibition at 50 mg L^{-1} and higher.

For the spherical TiO_2 ENMs (Figure 3d), only the TiO_2-NH_4^+ and TiO_2-PEG forms inhibited growth compared to controls (ANOVA, $p < 0.05$), with the latter being more toxic. Neither the uncoated spherical TiO_2 ENM nor the bulk material were toxic. The same pattern of toxicity was observed with the tubular TiO_2 materials (compare Figure 3d and e). However, there was some evidence of a material-shape effect with the tubular TiO_2 being less toxic than the spherical form when toxicity was observed. Nanodiamonds generally had little or no effect on bacterial growth (Figure 3f), except for a statistically significant (ANOVA, $p < 0.05$), 20 % reduction or less in grown compared to the controls for the -COOH and PEG-coated forms at the highest test concentration. In stark contrast to all other materials, the MWCNTs had a statistically significant (ANOVA, $p < 0.05$) and positive effect to enhance bacterial growth (Figure 3g), with possible exception of the MWCNT-COOH material that initially reduced growth at concentration up to 50 mg L^{-1}, but enhanced growth at 100 mg L^{-1}.

Yield measurements and glucose utilisation

In Figure 4, absolute biomass and growth yield are displayed for the CdTe QDs, spherical and tubular PEG-coated TiO_2 ENMs. For the QDs, the absence of biomass at the lethal doses was also reflected in zero carbon yields. At the sub-lethal doses of the QDs, a reduction in biomass with increasing test concentration was correlated to less measured carbon yield. For TiO_2 PEG-coated ENMs, the reduction in biomass at 100 mg L^{-1} (for both NPs and NTs), and also at 50 mg L^{-1} for NTs was reflected in a statistically significant reduction in measured yield relative to the growth control (ANOVA, $p < 0.05$).

Discussion

This work reports a modified MIC assay for determining the antibacterial effect of different commercial ENMs against the facultative microbe *E. coli* K-12 MG1655. For convenience and standardisation, the tests were carried out under fully oxic conditions in 96-well plates; and without the need for complex sonication procedures for different particles. The MIC assay was rapid, with good reproducibility and showed differential sensitivity according to the materials tested. The test method could resolve growth inhibition due to material-type (e.g., nano *versus* bulk material or metal salt) and also coating-effects within some ENMs.

The utility of the MIC assay for testing ENMs

The MIC assay used here is reasonably quick with incubations of only 12 hours (e.g., overnight). It is simplified for ENMs by not having a bespoke target for dispersion of the stock suspensions, but instead standardised stirring to facilitate sub-sampling of freshly prepared stocks for dosing. From a practical perspective, the use of a 50 % serial dilution based on nominal concentrations is sufficient to obtain reproducible results and the MIC values obtained can be used to rank materials in order of toxicity. For example, here the MIC assay remained responsive to non-essential toxic metals, as illustrated by the expected high toxicity of mercury and silver (Table 2), while identifying Ag NPs as less hazardous (see below on metals). It also correctly identified the low toxicity of the TiO_2 and MWCNTs (Table 2), in keeping with our previous environmental work on other organisms such as fish (TiO_2, Boyle et al., 2013; MWCNTs, Boyle et al., 2014). The MIC was able to identify CdTe quantum dots as toxic, but also differentiate the hazard of coatings and the bulk material (see below). The assay therefore clearly has utility as for identifying materials of concern.

The test medium in the MIC assay used here is a defined salt solution that can be inoculated. Furthermore, since both the bacteria and the ENMs tend to settle in the high ionic strength medium used (as expected by DLVO theory, see Handy et al., 2008), the test organism remains exposed to the test substance. It is there not useful (or relevant) to collect media samples directly from the plates, as this would not reflect the true exposure at the bottom of the test wells. The MIC screening method is therefore not reliant on 'water column' concentrations of the test substance being maintained as in *Daphnia* or fish embryo tests (Shaw et al., 2016), or other routine ecotoxicity tests. In any event, the design used here also included turbidity controls on each plate so that the data is readily corrected for changes in optical density due to the particles.

Across the different materials studied, the reproducibility of the assay was not affected by the surface coating of the materials, or by testing the uncoated forms, the bulk or the equivalent metal salts. In terms of precision and accuracy, the MIC assay generally provided a consistent reproducible output across the different materials tested with coefficient of variation (CV) within all experiments of less than 10 %. MWCNTs presented the largest variability in the calculated percentage CVs (>15 %). The uncoated MWCNTs were especially poorly dispersed in the saline medium (visually observed). Given the hydrophobic nature of MWCNTs, some difficulty in solution handling is expected. However, adding positive or negative coatings to the MWCNT did

not resolve this problem. The use of appropriate dispersing agents for MWCNTs could improve the solution handling and reproducibility for these materials, but the use of dispersing agents are discouraged in the ecotoxicity testing strategy (see Handy et al., 2012).

The regulatory acceptance of any growth inhibition assay will require a demonstration of optimal growth conditions to ensure the protocol has maximum sensitivity and that the organisms are healthy at the start of the experiment. The microplates, volumes used, and the media were found to be sufficiently robust for the MIC assay. The density of biomass and yield for the growth of the controls (Figure 4) in the absence of any test suspensions were in accordance to, in-house, previously determined figures for this strain of *E. coli* K-12 MG1655. The bacterium was able to grow in the presence of various metal ions, and at elevated metal concentrations. The conditions in our experiments also ensured that glucose was not limiting to microbial growth, and thus the inhibitory effects of the substances reported above are associated with chemical/nanomaterial toxicity.

Overall, the MIC assay presented here has utility as a first tier or rapid bacterial ecotoxicity test to identify materials of concern. The utility comes from the simplicity, speed and reproducibility of the test; the inclusion of a Hg positive control; the ability to correctly identify ENMs as toxic or of low hazard (i.e., no false negatives); as well as differentiating coating-effects and metal salt-effects where toxicity occurs. This MIC assay could identify ENMs of concern, before proceeding to the relevant OECD aquatic toxicity or soil organism tests in the overall testing strategy. Qiu et al. (2017) even suggest that a modified MIC assay followed by gene expression could be a first tier in high-throughput screening assays for ENMs.

Toxicity of ENMs compared to dissolved metals

One concern for risk assessment is whether ENMs are more toxic than their equivalent metal salts, and thus might require additional regulation for environmental protection. In this study, mercuric chloride was used as a positive control because of its established toxicity to *E. coli* K-12 (Boden and Murrell, 2011), and the metal completely inhibited growth compared to unexposed controls as expected. Silver nitrate was also extremely toxic with an MIC value of 1.5 mg L^{-1} (Table 2), similar to MIC values previously reported for Ag (7.1 mg L^{-1}, see Bondarenko et al., 2013). In contrast to the Hg and Ag salts, $CdCl_2$ were not toxic (Figure 3c) and $CuSO_4$ only inhibited growth at Cu concentrations of 50 mg L^{-1} or higher (Figure 3b). These observations are in keeping with the

homeostatic control of both Cu and Cd via the P-type ATPases in *E. coli* (Rensing et al., 2000). The K_2TeO_3 showed intermediate toxicity (Table 2), but with a clear concentration-dependent inhibition of growth (Figure 3c). The tellurium metal salt was much more toxic than $CdCl_2$ (Figure 3c). Both these metals (and the metals from CdTe QDs, see Dumas et al., 2010) can be used in the respiratory transport chain of microbes. Any Cd ions generated during electron transfer could presumably be excreted by the ATPase. However, the reduction of tellurite by the respiratory chain causes significant oxidative stress and toxicity to microbes (Trutko et al., 2000). Interestingly, the ability of *E. coli* to maintain energy production as measured by the yield per mole of carbon (glucose) consumed was confirmed for the CdTe QDs (Figures 4a-c). Regardless of the molecular explanations, the overall, the ranking of the metal salts in the MIC assay (Table 2) were as expected, and similar to previous rankings of metal toxicity to *E. coli* (Harrison et al., 2004).

There are also concerns that ENM toxicity may be imparted by metal ion dissolution from the surface of the material, resulting in dissolved metal toxicity. In the current study, this appears not to be the case. For example, the Ag NPs were the most toxic of the ENMs tested (Table 2; Figure 3a), but showed only a background dissolution of silver (Figure 2a). In any event, the trace Ag ions released would be rapidly chelated as insoluble AgCl in the NaCl-rich media (see Besinis et al., 2014). The Cu containing ENMs showed some dissolution (Figures 2d and e), with the highest rate of Cu release from the CuO-COOH form (3.67 $\mu g\ min^{-1}$, Table 1), but no toxicity was observed, except at one (high) concentration of the uncoated CuO ENMs (Figure 3b). In contrast, the bulk CuO stimulated growth (Figure 3b). This apparent hormesis is known for trace metals in *E. coli* and for Cu in several invertebrates; and possibly related to the early induction of metal resistance mechanisms in the cells (Stebbing, 1982). However, why this was observed with the bulk material and not the CuO ENMs is unclear.

The CdTe-QDs showed some toxicity with the ranking for the coating being $-NH_4^+$ > -COOH > -PEG (Table 2). Although some dissolution of both Cd and Te was measured in the $\mu g\ l^{-1}$ range from the dialysis experiments (Figures 2b and c; Table 1), the releases were not in the same order as the toxicity ranking of the CdTe QDs, suggesting dissolution was not the explanation. Regardless, for Cd dissolution, any metal release could not easily explain the toxicity of the QDs as $CdCl_2$ was not toxic in the experimental conditions here (Table 2). For the Te component of the CdTe QDs, the QDs were more potent in bacterial growth inhibition than the tellurium metal salt (Figure 3, Table 2), suggesting that dissolved tellurium species cannot explain

533 the observed QD toxicity. Unfortunately, there is only limited information on the mechanisms of
534 toxicity of Te to microbes (review, Lemire et al., 2013). Nonetheless, the most toxic form of the
535 QDs was the CdTe-NH_4^+ (Figure 3c) with an MIC value of 6 mg L^{-1} nominal concentration (0.03
536 mM Cd, 0.01 mM Te) (Table 2). One other study reports an MIC value for a different composition
537 of CdTe QDs at 10 nM for *E. coli* K-12 MG1655 (Schneider et al., 2009).
538
539 ***Particle size and coating effects***
540 The notion that particle size may influence toxicity has been widely debated and the environmental
541 concern is that substances of the same chemical composition may be more toxic at the nano scale
542 (Klaine et al., 2012). In the present study, the ENMs that showed toxicity (Ag NPs and the CdTe
543 QDs) were all more toxic than their bulk material counterparts (Table 2). For example, the MIC
544 values for Ag NPs and the (bulk) colloidal silver were 12 and 50 mg L^{-1} respectively (i.e., the ENM
545 was approximately 5 fold more toxic). The observed differences in the MIC values for Ag NPs
546 cannot be explained by metal ion dissolution for the reasons above. In the case of the CdTe bulk
547 material, no dissolution of either Cd or Te was observed (Figures 2b and c). However, direct
548 contact toxicity where the particles settle onto the surface of the microbes (see Reidy et al., 2013)
549 is possible. Interferences from other colloids in the media prevented the determination of the
550 particle number concentrations directly in the NaCl-EBS medium, but particle settling was
551 observed by eye during the experiments. In the case of the Ag NPs and colloidal silver, the particles
552 and the bacteria sank to the bottom of the test plate wells together. Similar observations were made
553 for the QDs, but with clearly faster settling of the NH_4^+-coated QDs aggregates. It is likely that
554 this settling enhanced the direct particle exposure of the microbes. NTA was possible in the 0.90
555 % NaCl solution (Table 1). In theory, any contact toxicity with the bacteria would be a function of
556 the aggregate size and particle number concentration. Interestingly for the Ag bulk material in 0.90
557 % NaCl, there were fewer much larger aggregates than that of the Ag NPs, representing about a 5
558 fold increase of silver settling in the micron dispersion which was coincident with the increase in
559 toxicity.
560 One central idea in the direct contact toxicity hypothesis of ENMs is that the particle
561 coating imparts some chemical reactivity (i.e., toxicity) and/or bioavailability to the surface of the
562 organism. Consequently, the type of surface coating may inform on toxicity, or influence the
563 dispersion in such a way as to alter the exposure. In the present study, the surface coatings were

564 chosen to represent positive, neutral and negative charges. The surface ligands of the coatings
565 studied (-COOH, -NH_4^+, -NH_2, -PEG) are not inherently toxic to microbes, and are found widely
566 in nature (Scott, 1968). Overall, there were no consistent trends of toxicity by surface-coating
567 across the materials tested. The data does not support the general idea that toxicity is driven by the
568 surface coating of the ENM. The only ENM that showed a clear coating-dependent effect on
569 toxicity was the CdTe-QDs, with the -NH_4^+ coating being the most toxic. However, the NTA in
570 0.90 % NaCl did not reveal any inherent trends in the aggregation behaviour of the different
571 coatings that might explain this toxicity (Table 1). The results of the dialysis experiments (Figure
572 2) showed that the type of coating did influence the dissolution for both the coated CuO ENMs
573 and the CdTe QDs; but this was not correlated with toxicity within the materials. For example, in
574 both types of ENMs, the -COOH coating gave the greatest maximum dissolution rates (Table 1),
575 but the -COOH coatings were not the most toxic (Table 2).
576 Finally, there are also concerns about particle shape, especially with high aspect ratio
577 nanomaterials (Donaldson et al., 2010). In the present study, both TiO_2 particles and TiO_2
578 nanotubes were examined. The spherical TiO_2-PEG material showed greater toxicity than the
579 nanotube form of the same material (compare Figures 3d and e). This difference in toxicity cannot
580 be attributed to dissolution of Ti metal (not observed). However, even considering the limitations
581 of NTA measurements with non-spherical particles, the spherical form made a greater number of
582 larger aggregates than the equivalent TiO_2-PEG nanotube (Table 1), tentatively suggesting that
583 settling behaviour contributed to this difference in toxicity arising from particle shape. Whatever
584 the mechanism, both the spherical and nanotube forms decreased the yield per mole of carbon
585 consumed (Figures 4d and e), suggesting interference with electron transfer in the respiratory
586 chain. How this occurs and why the spheres had the strongest effect on yield of the two materials
587 requires further investigation.
588

589 ***Conclusions and recommendations***

590 This study has demonstrated the utility of a modified MIC assay that can detect the toxicity of a
591 wide variety of ENMs with different surface-coatings, metal salts, and bulk materials; then rank
592 them accordingly. The test method achieves many of the practical goals for routine use in
593 regulatory ecotoxicology, being robust and with good reproducibility. The method is rationalised
594 so that detailed and bespoke sample preparation is not required for each ENM, and particle settling

595 in the 96-well plate technique used here does not confound the exposure (low risk of false
596 negative). Our recommendation is that the modified MIC assay can be adopted as a first tier in an
597 ecotoxicity testing strategy for ENMs, and of the materials studied, the Ag NPs and CdTe QDs are
598 identified as priority substances of concern.
599
600 **Acknowledgements**
601 Kind thanks to Dr Lee P. Hutt for assistance with growth yield methodologies. Dr Alexey Kalachev
602 (PlasmaChem GmbH, www.plasmachem.com) provided most of the coated-ENMs and their
603 associated core materials. The MWCNTs were provided by Dr Julie Muller of Nanocyl
604 (http://www.nanocyl.com/) and the MWCNT-PEG-coatings added at the University of
605 Manchester via Zahraa Al-ahmady.
606
607
608 **Declaration of interest**
609 This work was funded by the European Commission, under grant agreement FP7-309329
610 (NANOSOLUTIONS), with RDH as the principle investigator at UoP. The authors report no
611 conflicts of interest. The authors alone are responsible for the content and writing of the paper.
612
613 **References**

614 Besinis, A., De Peralta, T., Handy, R.D., 2014. The antibacterial effects of silver, titanium
615 dioxide and silica dioxide nanoparticles compared to the dental disinfectant chlorhexidine on
616 *Streptococcus mutans* using a suite of bioassays. Nanotoxicology. 8, 1-16.
617 Boden, R., Kelly, D.P., Murrell, J.C., Schäfer, H., 2010. Oxidation of dimethylsulfide to
618 tetrathionate by *Methylophaga thiooxidans* sp. nov.: a new link in the sulfur cycle.
619 Environmental Microbiology. 12, 2688-2699.
620 Boden, R., Murrell, J.C., 2011. Response to mercury (II) ions in *Methylococcus capsulatus*
621 (Bath). FEMS Microbiol. Lett. 324, 106-110.
622 Boden, R., Thomas, E., Savani, P., Kelly, D.P., Wood, A.P., 2008. Novel methylotrophic
623 bacteria isolated from the River Thames (London, UK). Environmental Microbiology. 10,
624 3225-3236.

625 Bondarenko, O., Juganson, K., Ivask, A., Kasemets, K., Mortimer, M., Kahru, A., 2013. Toxicity
626 of Ag, CuO and ZnO nanoparticles to selected environmentally relevant test organisms and
627 mammalian cells in vitro: a critical review. Archives of Toxicology. 87, 1181-1200.
628 Boyle, D., Al-Bairuty, G.A., Henry, T.B., Handy, R.D., 2013. Critical comparison of
629 intravenous injection of TiO_2 nanoparticles with waterborne and dietary exposures concludes
630 minimal environmentally-relevant toxicity in juvenile rainbow trout *Oncorhynchus mykiss*.
631 Environmental Pollution. 182, 70-79.
632 Boyle, D., Fox, J.E., Akerman, J.M., Sloman, K.A., Henry, T.B., Handy, R.D., 2014. Minimal
633 effects of waterborne exposure to single-walled carbon nanotubes on behaviour and
634 physiology of juvenile rainbow trout (*Oncorhynchus mykiss*). Aquatic Toxicology. 146, 154-
635 164.
636 Bradford, A., Handy, R.D., Readman, J.W., Atfield, A., Mühling, M., 2009. Impact of silver
637 nanoparticle contamination on the genetic diversity of natural bacterial assemblages in
638 estuarine sediments. Environmental Science and Technology. 43, 4530-4536.
639 Brennan, F.P., Grant, J., Botting, C.H., Flaherty, V., Richards, K.G., Abram, F., 2013. Insights
640 into the low-temperature adaptation and nutritional flexibility of a soil-persistent *Escherichia*
641 *coli*. FEMS Microbiology Ecology. 84, 75-85.
642 Coleman, D.C., Crossley, D.A., Hendrix, P.F., 2004. Fundamentals of soil ecology (2nd ed.).
643 Amsterdam, Boston: Elsevier Academic Press.
644 Crane, M., Handy, R.D., Garrod, J., Owen, R., 2008. Ecotoxicity test methods and environmental
645 hazard assessment for engineered nanoparticles. Ecotoxicology. 17, 421-437.
646 Donaldson, K., Murphy, F.A., Duffin, R., Poland, C.A., 2010. Asbestos, carbon nanotubes and
647 the pleural mesothelium: a review of the hypothesis regarding the role of long fibre retention
648 in the parietal pleura, inflammation and mesothelioma. Particle and Fibre Toxicology. 7, 5.
649 Dumas, E., Gao, C., Suffern, D., Bradforth, S.E., Dimitrijevic, N.M., Nadeau, J.L., 2010.
650 Interfacial charge transfer between CdTe quantum dots and gram negative vs gram positive
651 bacteria. Environmental Science and Technology. 44, 1464-1470.
652 Fajardo, C., Saccà, M.L., Costa, G., Nande, M., Martin, M., 2014. Impact of Ag and Al_2O_3
653 nanoparticles on soil organisms: In vitro and soil experiments. Science of the Total
654 Environment. 473-474, 254-61.

655 Gilbertson, L.M., Zimmerman, J.B., Plata, D.L., Hutchison, J.E., Anastas, P.T., 2015. Designing
656 nanomaterials to maximize performance and minimize undesirable implications guided by
657 the principles of green chemistry. Chemical Society Reviews. 44, 5758-5777.
658 Guyer, M.S., Reed, R.R., Steitz, J.A., Low, K.B., 1981. Identification of a Sex-factor-affinity
659 Site in *E. coli* as γδ. Cold Spring Harbor Symposia on Quantitative Biology. 45, 135-140.
660 Handy, R.D., van den Brink, N., Chappell, M., Mühling, M., Behra, R., Dušinská, M., Simpson,
661 P., Ahtiainen, J., Jha, A.N., Seiter, J., Bednar, A., Kennedy, A., Fernandes, T.F., Riediker,
662 M., 2012. Practical considerations for conducting ecotoxicity test methods with
663 manufactured nanomaterials: what have we learnt so far? Ecotoxicology. 21, 933-972.
664 Harrison, J.J., Ceri, H., Stremick, C.A., Turner, R.J., 2004. Biofilm susceptibility to metal
665 toxicity. Environmental Microbiology. 6, 1220-1227.
666 Hayashi, K., Morooka, N., Yamamoto, Y., Fujita, K., Isono, K., Choi, S., Ohtsubo, E., Baba, T.,
667 Wanner, B.L., Mori, H., Horiuchi, T., 2006. Highly accurate genome sequences of
668 *Escherichia coli* K-12 strains MG1655 and W3110. Molecular Systems Biology. 2, 1-5.
669 Kelly, D.P., Syrett, P.J., 1964. The effect of uncoupling agents on carbon dioxide fixation by a
670 *Thiobacillus*. Journal of General Microbiology. 34, 307-317.
671 Klaine, S.J., Koelmans, A.A., Horne, N., Carley, S., Handy, R.D., Kapustka, L., Nowack, B., von
672 der Kammer, F., 2012. Paradigms to assess the environmental impact of manufactured
673 nanomaterials. Environmental Toxicology and Chemistry. 31, 3-14.
674 Lead, J.R., Batley, G.E., Alvarez, P.J.J., Croteau, M-N., Handy, R.D., McLaughlin, M.J., Judy,
675 J.D., Schirmer, K. 2018. Nanomaterials in the environment: Behavior, fate, bioavailability,
676 and effects – An updated review. Environmental Toxicology and Chemistry, in press.
677 DOI 10.1002/etc.4147
678 Lemire, J.A., Harrison, J.J., Turner, R.J., 2013. Antimicrobial activity of metals: mechanisms,
679 molecular targets and applications. Nature Reviews Microbiology. 11, 371-384.
680 Meesters, J.A.J., Quik, J.T.K., Koelmans, A.A., Hendriks, A.J., van de Meent, D., 2016.
681 Multimedia environmental fate and speciation of engineered nanoparticles: a probabilistic
682 modeling approach. Environmental Science Nano. 3, 715-727.
683 Morones, J.R., Elechiguerra, J.L., Camacho, A., Holt, K., Kouri, J.B., Ramírez, J.T., Yacaman,
684 M.J., 2005. The bactericidal effect of silver nanoparticles. Nanotechnology. 16, 2346-2353.

685 Mudunkotuwa, I.A., Anthony, T.R., Grassian, V.H., Peters, T.M., 2016. Accurate quantification
686 of TiO_2 nanoparticles collected on air filters using a microwave-assisted acid digestion
687 method. Journal of Occupational and Environmental Hygiene. 13, 30-39.
688 Oomen, A.G., Bos, P.M.J., Fernandes, T.F., Hund-Rinke, K., Boraschi, D., Byrne, H.J.,
689 Aschberger, K., Gottardo, von der Kammer, S.F., Kuhnel, D., Hristozov, D., Marcomini, A.,
690 Migliore, L., Scott-Fordsmand, J., Wick, P., Landseidel, R., 2014. Concern-driven integrated
691 approaches to nanomaterial testing and assessment – report of the NanoSafety Cluster
692 Working Group 10. Nanotoxicology. 8, 334-348.
693 Owen, R., Crane, M., Grieger, K., Handy, R.D., Linkov, I., Depledge, M., 2009. Strategic
694 approaches for the management of environmental risk uncertainties posed by nanomaterials.
695 Nanomaterials: Risks and Benefits 369-384. Netherlands: Springer.
696 Pirt, S.J., 1967. A Kinetic Study of the Mode of Growth of Surface Colonies of Bacteria and
697 Fungi. Microbiology. 47, 181-197.
698 Qiu, T.A., Nguyen,T.H.T., Hudson-Smith, N.V., Clement, P.L., Forester, D.C., Frew, H., Hang,
699 M.N., Murphy, C.J., Hamers, R.J., Feng, Z.V., Haynes, C.L., 2017. Growth-based bacterial
700 viability assay for interference-free and high-throughput toxicity screening of nanomaterials.
701 Analytical Chemistry. 89, 2057.
702 Reidy, B., Haase, A., Luch, A., Dawson, K.A., Lynch, I., 2013. Mechanisms of silver
703 nanoparticle release, transformation and toxicity: A critical review of current knowledge and
704 recommendations for future studies and applications. Materials. 6, 2295-2350.
705 Reinsch, B.C., Levard, C., Li, Z., Ma, R., Wise, A., Gregory, K.B., Brown, G.E., Lowry, G.V.,
706 2012. Sulfidation of silver nanoparticles decreases *Escherichia coli* growth inhibition.
707 Environmental Science and Technology. 46, 6992-7000.
708 Rensing, C., Fan, B., Sharma, R., Mitra, B., Rosen, B. P., 2000. CopA: An *Escherichia coli*
709 Cu(I)-translocating P-type ATPase. Proceedings of the National Academy of Sciences. 97,
710 652-656.
711 Schneider, R., Wolpert, C., Guilloteau, H., Balan, L., Lambert, J., Merlin, C., 2009. The
712 exposure of bacteria to CdTe-core quantum dots: the importance of surface chemistry on
713 cytotoxicity. Nanotechnology. 20, 225101.
714 Scott, J. E., 1968. Ion binding in solutions containing mucopolysaccharides. In: The Chemical
715 Physiology of Mucopolysaccharides, (G. Quintarelli, ed.), Churchill, London, 171-178.

716 Shaw, B.J., Liddle, C.C., Windeatt, K.M., Handy, R.D., 2016. A critical evaluation of the fish
717 early-life stage toxicity test for engineered nanomaterials: experimental modifications and
718 recommendations. Archives of Toxicology. 90, 2077-2107.
719 Shaw, B.J., Ramsden, C.S., Turner, A., Handy, R.D., 2013. A simplified method for determining
720 titanium from TiO_2 nanoparticles in fish tissue with a concomitant multi-element analysis.
721 Chemosphere. 92, 1136-1144.
722 Stebbing, A.R.D., 1982. Hormesis-the stimulation of growth by low levels of inhibitors. The
723 Science of the Total Environment. 22, 213-234.
724 Taurozzi, J.S., Hackley, V.A., Wiesner, M.R., 2010. Ultrasonic dispersion of nanoparticles for
725 environmental, health and safety assessment – issues and recommendations. Nanotoxicology.
726 5, 711-729.
727 Trutko, S.M., Akimenko, V.K., Suzina, N.E., Anisimova, L.A., Shlyapnikov, M.G., Baskunov,
728 B.P., Duda, V.I., Boronin, A.M., 2000. Involvement of the respiratory chain of gram-
729 negative bacteria in the reduction of tellurite. Archives of Microbiology. 173, 178-186.
730 Tuovinen, O., Kelly, D., 1973. Studies on the growth of *Thiobacillus ferrooxidans*. I. Use of
731 membrane filters and ferrous iron agar to determine viable numbers, and comparison with 14
732 CO_2 -fixation and iron oxidation as measures of growth. Archiv für Mikrobiologie. 88, 285-
733 298.
734 Wiegand, I., Hilpert, K., Hancock, R.E., 2008. Agar and broth dilution methods to determine the
735 minimal inhibitory concentration (MIC) of antimicrobial substances. Nature Protocols. 3,
736 163-175.
737 Winfield, M.D., Groisman, E.A., 2003. Role of nonhost environments in the lifestyles of
738 *Salmonella* and *Escherichia coli*. Applied and Environmental Microbiology. 69, 3687.
739 Xiu, Z., Liu, Y., Mathieu, J., Wang, J., Zhu, D., Alvarez, P.J.J., 2014. Elucidating the genetic
740 basis for *Escherichia coli* defense against silver toxicity using mutant arrays. Environmental
741 Toxicology and Chemistry. 33, 993-997.
742 Yoon, K.Y., Hoon Byeon, J., Park, J.H., Hwang, J., 2007. Susceptibility constants of *Escherichia*
743 *coli* and *Bacillus subtilis* to silver and copper nanoparticles. Science of the Total
744 Environment. 373, 572-575.
745

Table 1. Characterisation of the stock suspensions and solutions in 0.90 % NaCl and in the NaCl-EBS medium, at the highest nominal test concentration of 100 mg L^{-1}.

Material (Supplier)	****Manufacturer's information	*Mean aggregate size in 0.90 % NaCl (nm)	*Mean particle concentration in 0.90 % NaCl (x10^8 particles mL^{-1})	Calculated total metal concentration in NaCl-EBS medium		**Measured metal concentration in NaCl-EBS medium (mg L^{-1})	***Metal dissolution rate (µg min^{-1})
				(mg L^{-1})	(mM)		
Ag Bulk, CAS 7440-22-4 (Sigma-Aldrich 327085, Lot MKBR8201V)	Diameter, 2 - 3.5 µm; purity ≥ 99.9 % trace metal basis	198.33 ± 57.67	0.33 ± 0.03	84.3 Ag	0.77 Ag	0.42 Ag	< 0.01 Ag
Ag NPs, with PVP dispersant, CAS 7440-22-4 (Sigma-Aldrich 576832, Lot 7721KH)	Diameter, < 100 nm; purity, 99.5 % trace metals basis; Fisher sub-sieve sizer surface area, 5.0 m^2 g^{-1}	87.33 ± 2.4	3.72 ± 0.16	84.5 Ag	0.77 Ag	3.71 Ag	0.02 Ag
$AgNO_3$, CAS 7761-88-8 (BDH Chemicals)	0.10 M volumetric solution, certified	--	--	88.8 Ag	0.83 Ag	9.00 Ag	0.04 Ag
CuO Bulk, CAS 1317-38-0 (British Drug Houses Ltd)	Analar grade	258.67 ± 12.72	4.31 ± 0.96	66.4 Cu	1.05 Cu	55.54 ± 3.81 Cu	1.54 Cu
#CuO NPs uncoated, CAS 1317-38-0 (PlasmaChem GmbH, Lot YF1309121)	Diameter, 10 - 20 nm; surface area, 42 ± 2 m^2 g^{-1}	182.33 ± 13.38	3.06 ± 0.79	66.4 Cu	1.05 Cu	59.71 ± 1.82 Cu	3.42 Cu
#CuO NPs COOH-coated, CAS 1317-38-0 (PlasmaChem GmbH, Lot YF140114)	Diameter, 10 - 20 nm; surface area, 7.4 ± 0.5 m^2 g^{-1}	135.33 ± 31.55	1.60 ± 0.43	35.69 Cu	0.56 Cu	31.18 ± 0.47 Cu	3.67 Cu
#CuO NPs NH_4^+-coated, CAS 1317-38-0 (PlasmaChem GmbH, Lot 140114)	Diameter, 10 - 20 nm; surface area, 6.1 ± 0.5 m^2 g^{-1}	120.33 ± 32.33	1.82 ± 0.08	43.16 Cu	0.67 Cu	41.51 ± 1.11 Cu	1.81 Cu

#CuO NPs PEG-coated, CAS 1317-38-0 (PlasmaChem GmbH, Lot YF140114)	Diameter, 10 - 20 nm	126.33 ± 9.26	1.13 ± 0.23	24.07 Cu	0.38 Cu	22.26 ± 0.02 Cu	2.00 Cu
$CuSO_4.5H_2O$, CAS 7758-99-8 (Sigma-Aldrich 31293 , Lot SZBC0170V)	Purity, 99 - 102 %	--	--	65.5 Cu	1.03 Cu	57.90 ± 0.26 Cu	3.71 Cu
CdTe Bulk, CAS 1306-25-8 (Sigma-Aldrich 256544, Lot MKBK6448V)	Diameter, < 250 µm; purity, ≥ 99.99 % trace metal basis	116.67 ± 17.48	0.77 ± 0.03	39.3 Cd 44.3 Te	0.35 Cd 0.35 Te	12.77 ± 0.82 Cd 14.28 ± 1.03 Te	< 0.01 Cd < 0.01 Te
#CdTe QDs COOH-coated, CAS 1306-25-8 (PlasmaChem GmbH, Lot YF140402)	Diameter, 3 -5 nm	76.67 ± 2.19	10.66 ± 0.21	35.4 Cd 5.81 Te	0.31 Cd 0.016 Te	24.00 ± 0.60 Cd 3.99 ± 0.16 Te	4.31 Cd 4.41 Te
#CdTe QDs NH_4^+-coated, CAS 1306-25-8 (PlasmaChem GmbH, Lot YF140402)	Diameter, 3 -5 nm	65.33 ± 14.65	6.19 ± 1.61	52.1 Cd 28.3 Te	0.46 Cd 0.22 Te	33.92 ± 0.18 Cd 13.62 ± 0.26 Te	3.74 Cd 2.30 Te
#CdTe QDs PEG-coated, CAS 1306-25-8 (PlasmaChem GmbH, Lot YF140402)	Diameter, 3 -5 nm	157.33 ± 12.67	2.71 ± 0.07	49.5 Cd 9.23 Te	0.44 Cd 0.07 Te	28.99 ± 0.18 Cd 5.32 ± 0.07 Te	3.00 Cd 3.81 Te
$CdCl_2$, CAS 10108-64-2 (Sigma-Aldrich 202908, Lot MKBM1769)	Purity, 99.99 % trace metal basis	--	--	38.7 Cd	0.34 Cd	30.6 ± 0.14 Cd	6.97 Cd
K_2TeO_3, CAS 7790-58-1 (Hopkin and Williams Ltd)	97 % minimum K_2TeO_3	--	--	46.4 Te	0.36 Te	46.79 ± 1.38 Te	6.71 Te
TiO_2 Bulk, CAS 13463-67-7 (Acros Organics 277370010, Lot A0224336)	Purity, 98.0 - 100.5 %	301.00 ± 27.61	28.95 ± 2.75	51.83 Ti	1.08 Ti	35.57 ± 4.65 Ti	< 0.01 Ti
#TiO_2 NPs uncoated (PlasmaChem GmbH, Lot YF1310291)	Diameter, 10 -20 nm; surface area, 98 ± 10 $m^2 g^{-1}$	36.00 ± 1.15	4.66 ± 0.50	51.83 Ti	1.08 Ti	31.14 ± 1.36 Ti	< 0.01 Ti

#TiO_2 NPs COOH-coated, (PlasmaChem GmbH, Lot YF140402)	Diameter, 10 - 20 nm	186.67 ± 21.11	0.72 ± 0.17	^	^	^^	^^
#TiO_2 NPs NH_4^+-coated (PlasmaChem GmbH, Lot YF140114)	Diameter, 10 - 20 nm	58.33 ± 12.45	3.24 ± 0.09	^	^	^^	^^
#TiO_2 NPs PEG-coated (PlasmaChem GmbH, Lot YF140402)	Diameter, 10 - 20 nm	145.00 ± 2.52	8.83 ± 0.97	^	^	^^	^^
#TiO_2 NTs uncoated (PlasmaChem GmbH, Lot YF140402)	Aspect ratio, 1:5; surface area, 123 ± 10 m^2 g^{-1}	24.67 ± 4.09	2.18 ± 0.34	51.83 Ti	1.08 Ti	15.55 ± 1.07 Ti	< 0.01 Ti
#TiO_2 NTs COOH-coated (PlasmaChem GmbH, YF140402)	Aspect ratio, 1:5; surface area, 20 ± 2 m^2 g^{-1}	54.33 ± 21.3	2.71 ± 0.38	^	^	^^	^^
#TiO_2 NTs NH_4^+-coated (PlasmaChem GmbH, Lot YF140402)	Aspect ratio, 1:5; surface area, 41 ± 4 m^2 g^{-1}	53.00 ± 7.1	3.55 ± 0.27	^	^	^^	^^
#TiO_2 NTs PEG-coated (PlasmaChem GmbH, Lot YF140402)	Aspect ratio, 1:5; surface area, 11 ± 1 m^2 g^{-1}	45.00 ± 11.72	3.16 ± 0.32	^	^	^^	^^
#Nanodiamonds COOH-coated, CAS 7782-40-3 (PlasmaChem GmbH, Lot YF1310311)	Diameter, 4 - 6 nm; surface area, 180 ± 15 m^2 g^{-1}	59.00 ± 5.57	4.71 ± 0.12	--	--	--	--
#Nanodiamonds NH_4^+-coated, CAS 7782-40-3 (PlasmaChem GmbH, Lot YF140114)	Diameter, 4 - 6 nm; surface area, 289 ± 10 m^2 g^{-1}	55.33 ± 17.03	2.98 ± 0.70	--	--	--	--
#Nanodiamonds PEG-coated, CAS 7782-40-3 (PlasmaChem GmbH, Lot YF140114)	Diameter, 4 - 6 nm; surface area, 244 ± 20 m^2 g^{-1}	68.00 ± 5.13	3.12 ± 0.23	--	--	--	--

[#]MWCNTs uncoated, CAS 308068-56-6 (Nanocyl 7000, Batch A2105)	Aspect ratio, 1:100; purity, 98 % carbon by weight; surface area, 213 ± 5 m^2 g^{-1}	28.67 ± 2.33	0.31 ± 0.04	--	--	--	--
[#]MWCNTs COOH-coated, CAS 308068-56-6 (Nanocyl 3151, Batch 131205)	Aspect ratio, 1:100; purity, 98 % carbon by weight; surface area, 284 ± 2 m^2 g^{-1}	42.33 ± 9.02	0.63 ± 0.17	--	--	--	--
[#]MWCNTs NH_2-coated, CAS 308068-56-6 (Nanocyl 3152, Batch 131205)	Aspect ratio, 1:100; purity, 98 % carbon by weight; surface area, 253 ± 10 m^2 g^{-1}	42.33 ± 7.22	0.42 ± 0.08	--	--	--	--
[#]MWCNTs PEG-coated, CAS 308068-56-6 (University of Manchester)	Aspect ratio, 1:100; purity, 98 % carbon by weight; surface area, 26 ± 3 m^2 g^{-1}	64.67 ± 14.84	4.00 ± 0.50	--	--	--	--
$HgCl_2$, CAS 7487-94-7 (Sigma-Aldrich M1136, Lot 071K1201)	Purity, 99 %	--	--	83.0 Hg	0.41 Hg	75.29 ± 0.21 Hg	^^

[#]Material supplied via the NANOSOLUTIONS Project; Quantum dots (QDs); Polyethylene glycol (PEG); Multi-walled carbon nanotubes (MWCNTs); Nanoparticles (NPs); Nanotubes (NTs); Polyvinylpyrrolidinone (PVP); *Data are the mean aggregate hydrodynamic diameters and mean particle concentration from particle size distribution measurements made by NTA using the Nanosight LM10. Values are mean ± standard error of the mean (S.E.M) (n = 3 measurements of the dispersion); **Data are means ± S.E.M (n = 3 replicates) of total measured metal concentration by ICP-OES; ***Dissolution rate calculated from dialysis experiments in triplicate; ****Unless otherwise stated, Brunauer–Emmett–Teller (BET) surface area values (mean ± one standard deviation, n = 3) provided *via* the NANOSOLUTIONS Project; --Data irrelevant to the chemical; ^Not possible to calculate from the manufacturers' information on material composition; ^^Not measured.

746

747

748

749

750 **Table 2.** Minimum inhibitory concentration (MIC) values in mg L^{-1}, following *Escherichia coli* K-12 MG1655 exposure to a dilution
751 series of the test materials with nominal concentrations of these materials from 1.5 to 100 mg L^{-1} in 96-well plates. '> 100' shows no
752 detection of a MIC value for that material at all the tested concentrations. '> 100 *' shows no detection of a MIC value for that
753 material at all the tested concentrations, with more than 20 % bacterial growth inhibition relative to the negative growth control at the
754 100 mg L^{-1} nominal test concentration, and statistical significant difference in absolute growth (biomass production in mg dry biomass
755 L^{-1}) from the normal growth control (ANOVA, $p < 0.05$) at the 100 mg L^{-1} nominal test concentration.

Chemical	ENMs uncoated	ENMs COOH-coated	ENMs NH_4^+-coated §	ENMs PEG-coated	Bulk form	Metal salt §§
Ag	12	--	--	--	50	1.5
CuO	> 100 *	> 100	> 100	> 100	> 100	> 100 *
CdTe	--	25	6	100	> 100	> 100 Cd 50 Te
Spherical TiO_2	> 100	> 100	> 100 *	> 100 *	> 100	--
Tubular TiO_2	> 100	> 100	> 100 *	> 100 *	> 100	--
Nanodiamonds	--	> 100 *	> 100	> 100	--	--
MWCNTs	> 100	> 100	> 100	> 100	--	--
Hg	--	--	--	--	--	1.5

Engineered nanomaterials (ENMs); carboxylate functional coating (COOH); ammonium functional coating (NH_4^+); polyethylene glycol functional coating (PEG); multi-walled carbon nanotubes (MWCNTs); § amine functional coating (NH_2) for MWCNTs only; §§ metal salts used were $AgNO_3$, $CuSO_4.5H_2O$, $CdCl_2$, K_2TeO_3, $HgCl_2$; -- not applicable.

756

757 Figure Legends

758 **Figure 1**. Particle size distribution (bin sizes are hydrodynamic diameter in nm) measured by
759 Nanoparticle Tracking Analysis (Nanosight LM10) of the cadmium telluride quantum dots; (a)
760 carboxylate-coated, (b) ammonium-coated, (c) polyethylene glycol-coated, at the 100 mg L^{-1}
761 nominal concentration in 0.90 % (*w/v*) NaCl. Data presented as mean ± S.E.M, from 3 sub-samples
762 of each prepared stock. Note, the particle number concentrations are x10^6 particles mL^{-1}

763 **Figure 2**. Dialysis curves showing the release of total dissolved metal ions from test
764 suspensions/solutions over a 24 h period when suspended in NaCl-EBS growth media at pH 6.5
765 for: (a) silver, (b) cadmium, (c) tellurium, (d) uncoated copper oxide, and (e) coated copper oxide
766 materials with their appropriate controls. The measured metal concentrations have been
767 normalised to a starting dialysis concentration of 100 mg L^{-1} of test material. Data are means ±
768 S.E.M (n = 3) separate beakers for each material type and control beakers. Curves were fitted using
769 a hyperbola, single rectangular, two parameter equation (SigmaPlot 13). Equations for the curve
770 fits are reported in the supplement (Table S1).

771 **Figure 3**. The effect of the different test material nominal concentrations on bacterial growth,
772 expressed as a percentage relative to the normal growth control (absence of test suspensions), using
773 the MIC assay for (a) silver, (b) copper, (c) cadmium telluride quantum dots, (d) spherical titanium
774 dioxide, (e) tubular titanium dioxide, (f) nanodiamonds, (g) MWCNTs. Data are mean ± S.E.M (n
775 = 6). Different letters indicate significant differences amongst the relative tested concentrations
776 (ANOVA, $p < 0.05$). Complete absence of letters means no statistical difference between the types
777 of material within the test. '*' refers to statistical significant difference in calculated biomass from
778 the growth control at that particular concentration.

779 **Figure 4**. Biomass (mg dry weight biomass L^{-1}) and growth yield (g per mole of carbon
780 consumed) from test materials exposure and normal growth control (no test suspension) for (a)
781 CdTe QDs COOH-coated, (b) CdTe QDs NH_4^+-coated, (c) CdTe QDs PEG-coated, (d) TiO_2 NPs
782 PEG-coated, (e) TiO_2 NTs PEG-coated. Statistical significant difference from the growth control
783 is represented with '*' for both biomass and yield with ANOVA, $p < 0.05$. Complete absence of
784 figure bars signifies no measurable biomass and/or yield.

Figure 1.

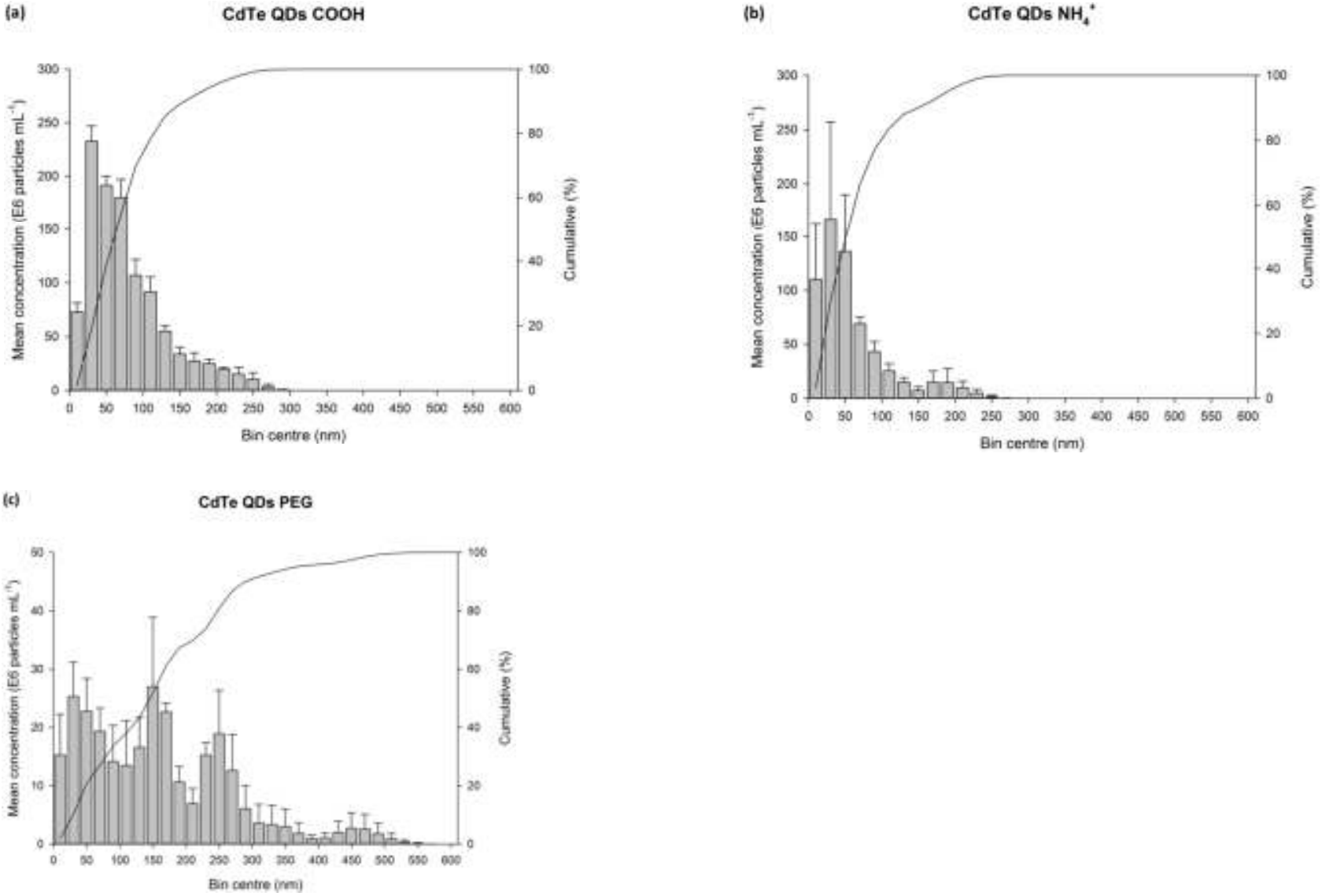
(a)
CdTe QDs COOH
Mean concentration (E6 particles mL-1)
Cumulative (%)
Bin centre (nm)
(b)
CdTe QDs NH4+
Mean concentration (E6 particles mL-1)
Cumulative (%)
Bin centre (nm)
(c)
CdTe QDs PEG
Mean concentration (E6 particles mL-1)
Cumulative (%)
Bin centre (nm)

800 **Figure 2.**

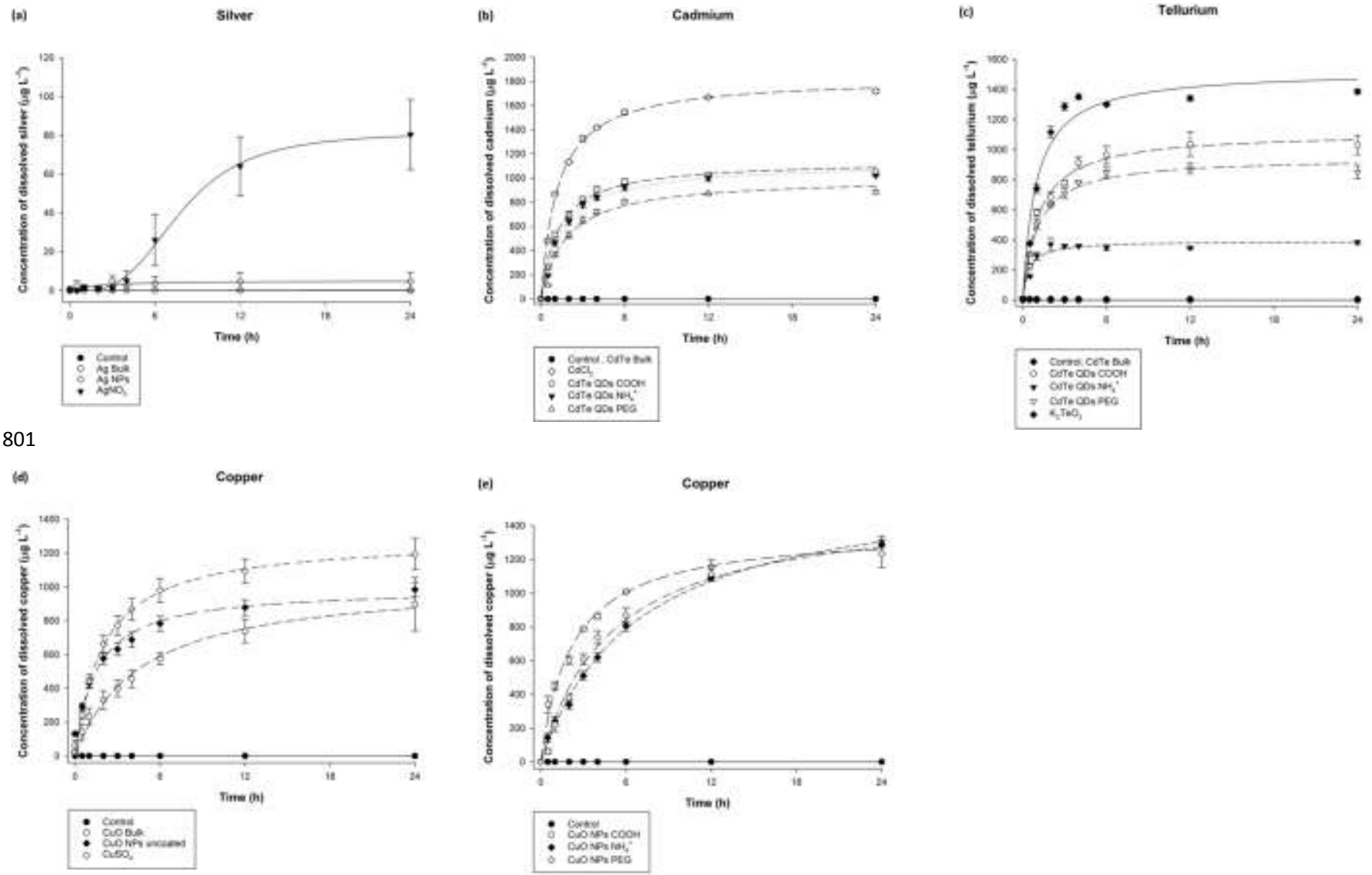

801

Figure 3.

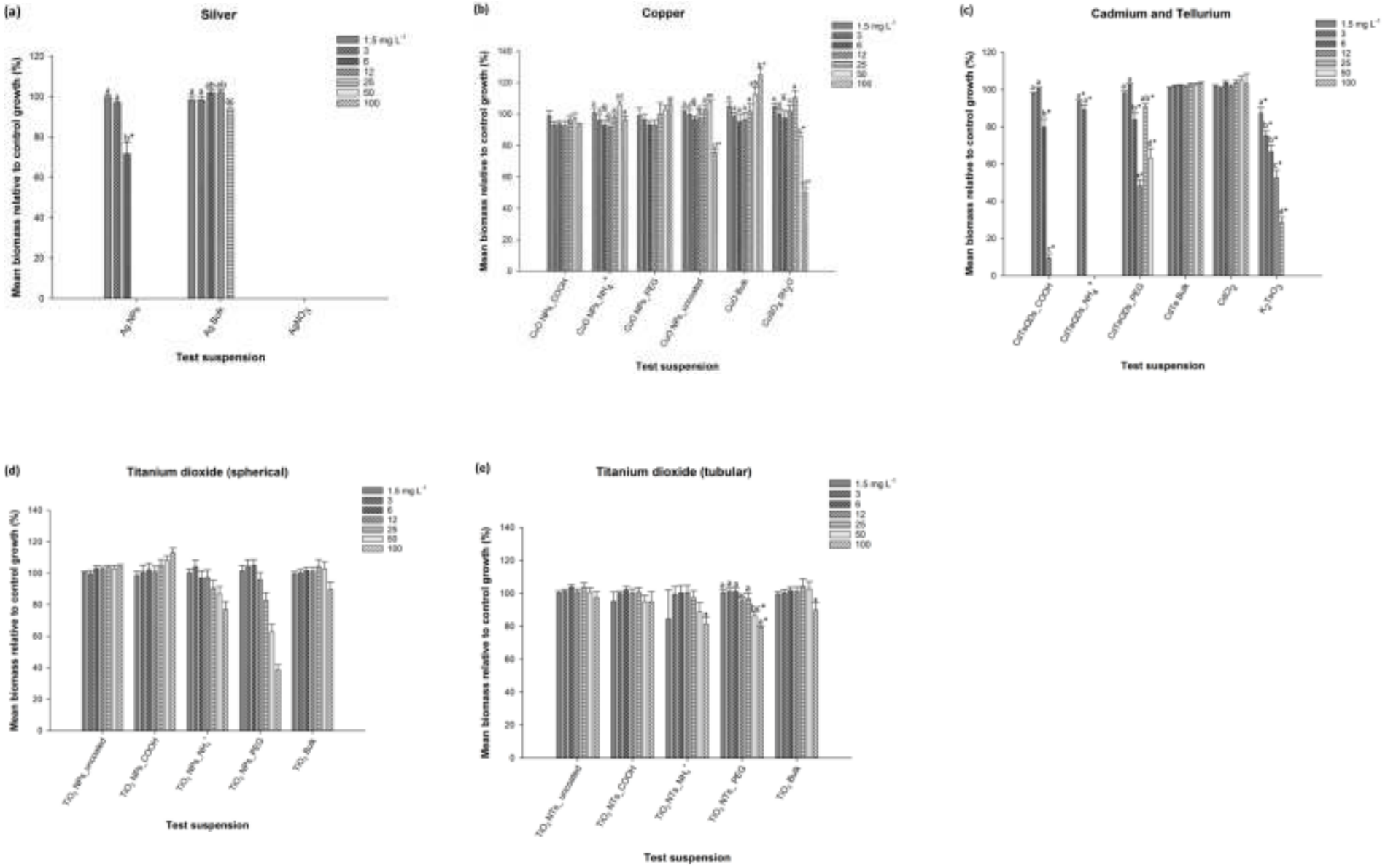
(a)
Silver
Mean biomass relative to control growth (%)
Test suspension
(b)
Copper
Mean biomass relative to control growth (%)
Test suspension
(c)
Cadmium and Tellurium
Mean biomass relative to control growth (%)
Test suspension
(d)
Titanium dioxide (spherical)
Mean biomass relative to control growth (%)
Test suspension
(e)
Titanium dioxide (tubular)
Mean biomass relative to control growth (%)
Test suspension

Figure 3. (cont.)

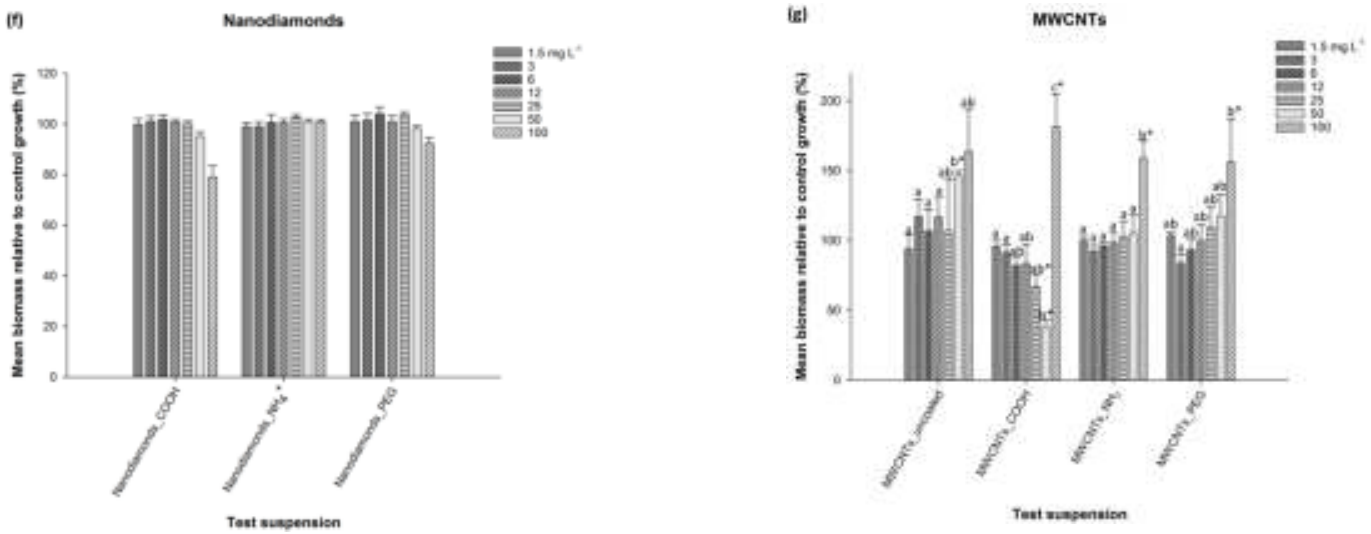

824 **Figure 4.**

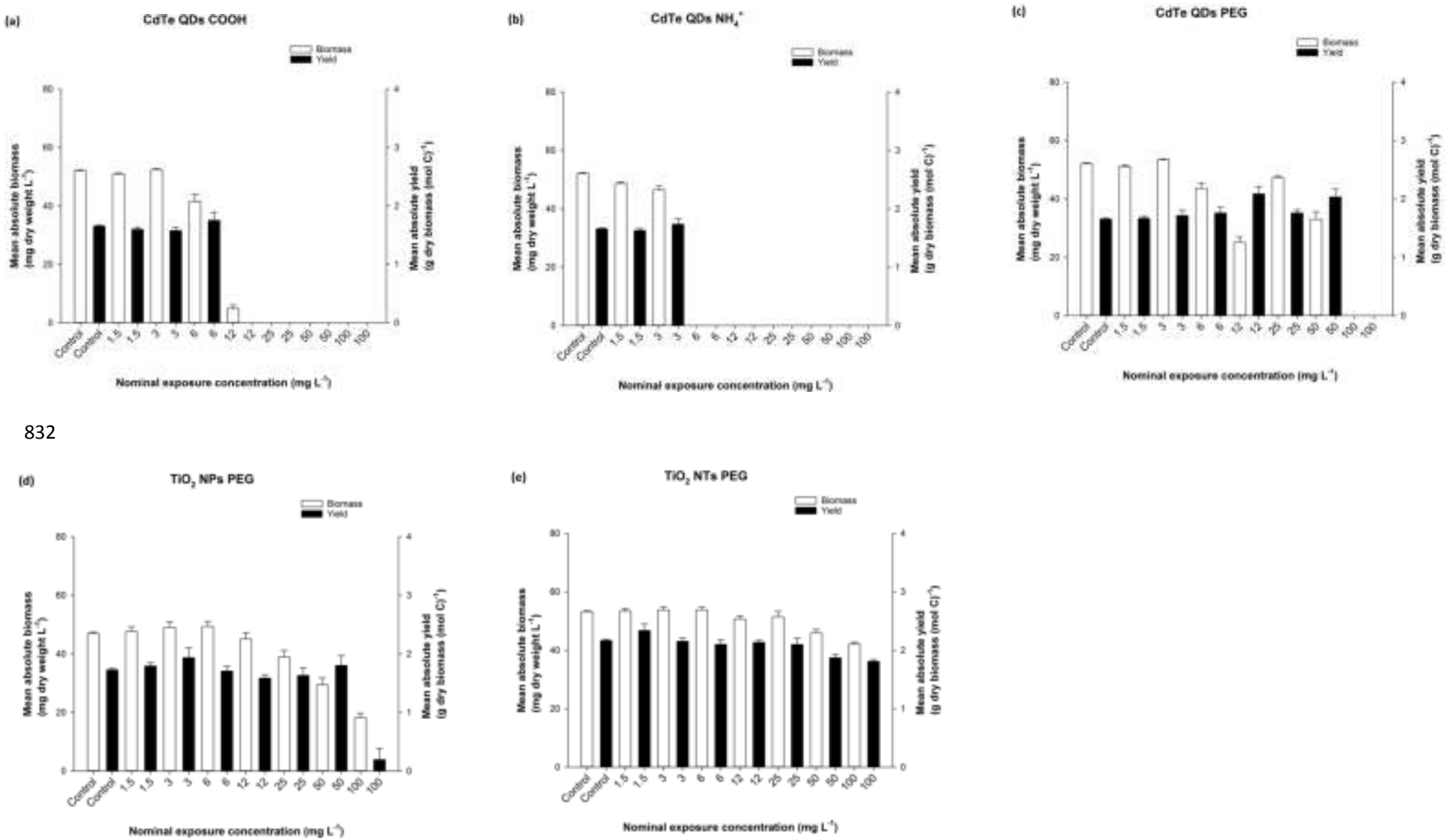

832